Electronic Supplementary Information

Hybrid Polymer Matrix Composite Containing Polyaniline and Nafion as Novel Precursor of the Enhanced Catalyst for Oxygen Reduction Reaction

Xudong Fu,[ab] Suli Wang,[a] Huanqiao Li,[a] Zhangxun Xia,[a] Luhua Jiang[a] and Gongquan Sun*[a]

[a] Division of Fuel Cell & Battery, Dalian National Laboratory for Clean Energy, Dalian Institute of Chemical Physics, Chinese Academy of Sciences, Zhongshan Road 457, Dalian 116023, China.

[b] University of Chinese Academy of Sciences, Beijing 100039, China.

* Corresponding author. Tel.: +86 411 84379063; fax: +86 411 84379063

E-mail address: gqsun@dicp.ac.cn (G. Sun)

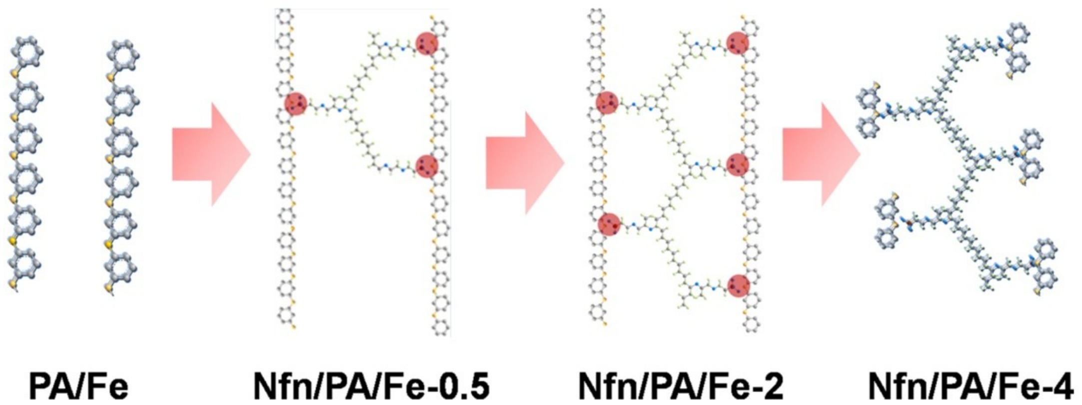

Scheme S1 Schematic representation of different mass ratios of Nafion to aniline.

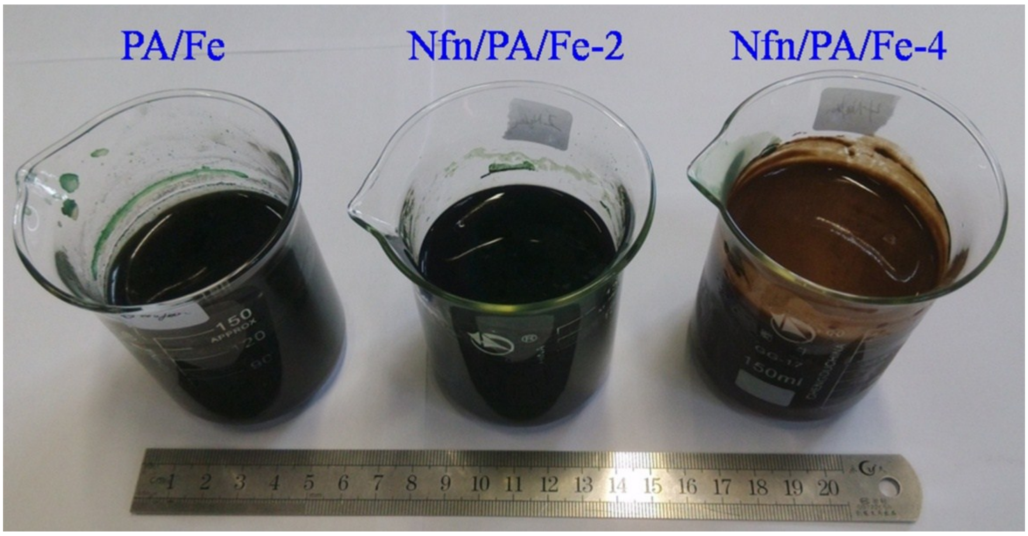

Fig. S1 Digital photographs of PA/Fe, Nfn/PA/Fe-2, Nfn/PA/Fe-4 after aniline polymerization for 36h.

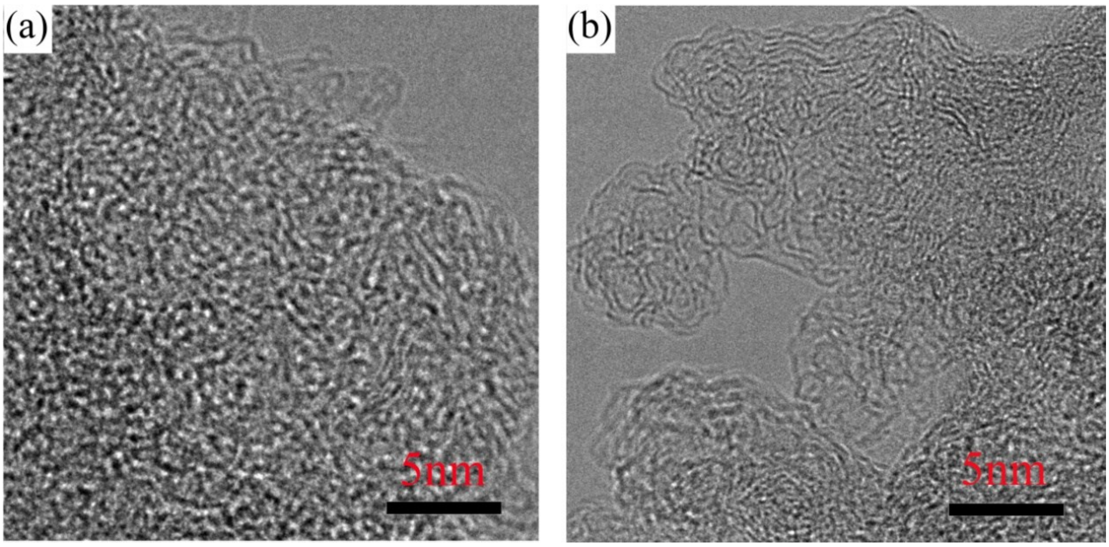

Fig. S2 TEM images of Nfn/PA-2 (a) and PA/Fe (b).

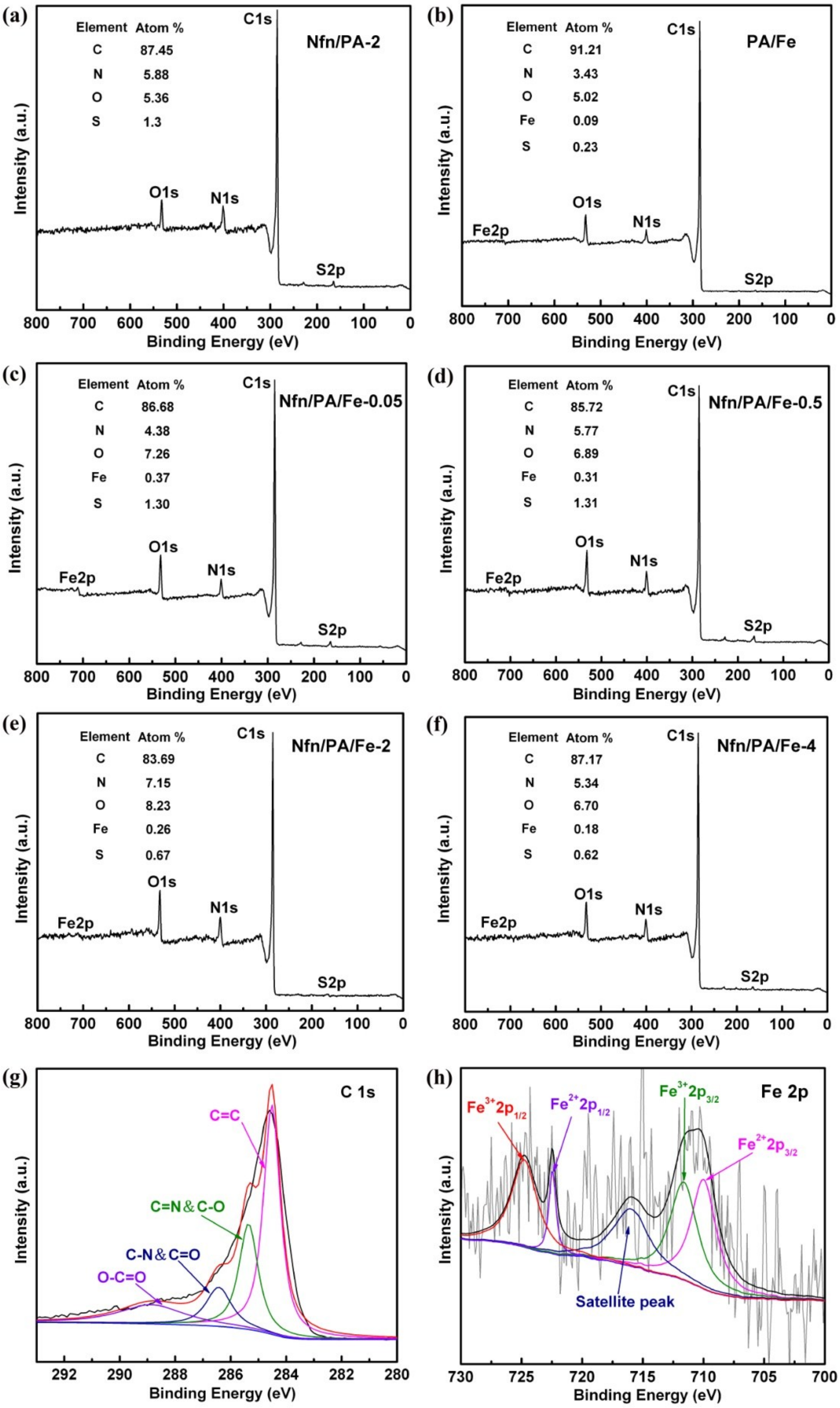

Fig. S3 XPS spectra of Nfn/PA-2 (a), PA/Fe (b), Nfn/PA/Fe-0.05 (c), Nfn/PA/Fe-0.5 (d), Nfn/PA/Fe-2 (e), Nfn/PA/Fe-4 (f) and C1s (g), Fe2p (h) spectra of Nfn/PA/Fe-2.

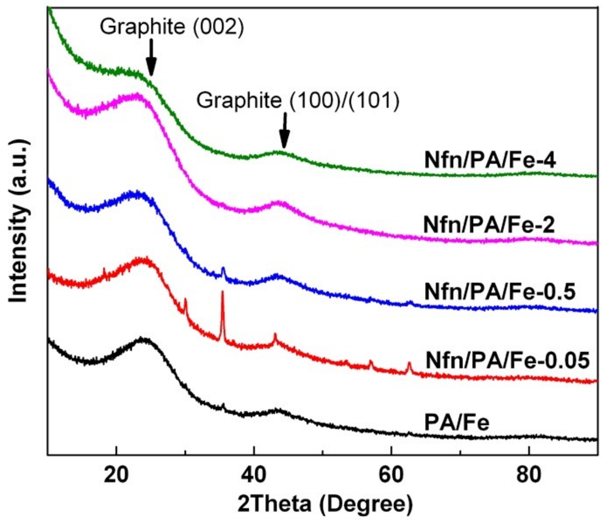

Fig. S4 XRD curves of PA/Fe, Nfn/PA/Fe-0.05, Nfn/PA/Fe-0.5, Nfn/PA/Fe-2, Nfn/PA/Fe-4 (after pyrolysis).

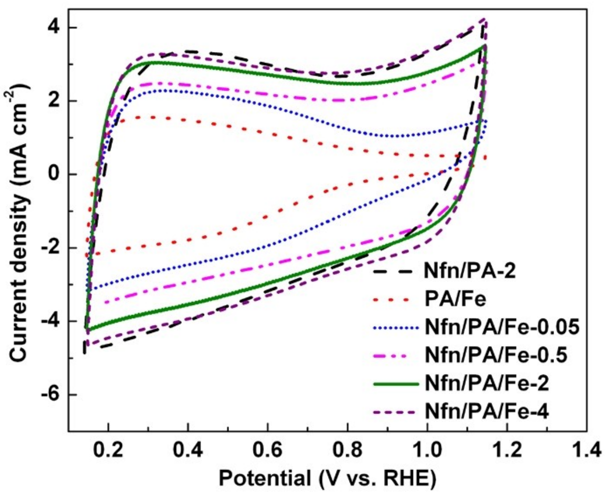

Fig. S5 CV curves of Nfn/PA-2, PA/Fe, Nfn/PA/Fe-0.05, Nfn/PA/Fe-0.5, Nfn/PA/Fe-2, Nfn/PA/Fe-4.

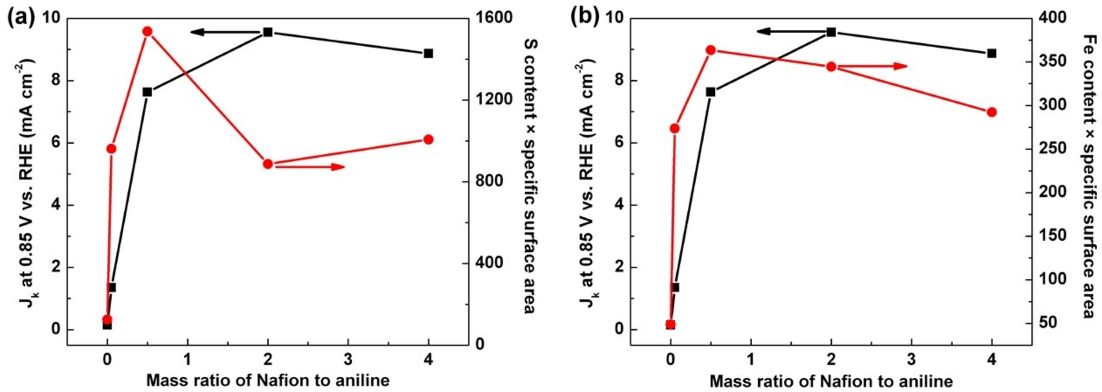

Fig. S6 Relationship between kinetic current densities of prepared catalysts and the amounts of accessible sulfur (a), iron (b).

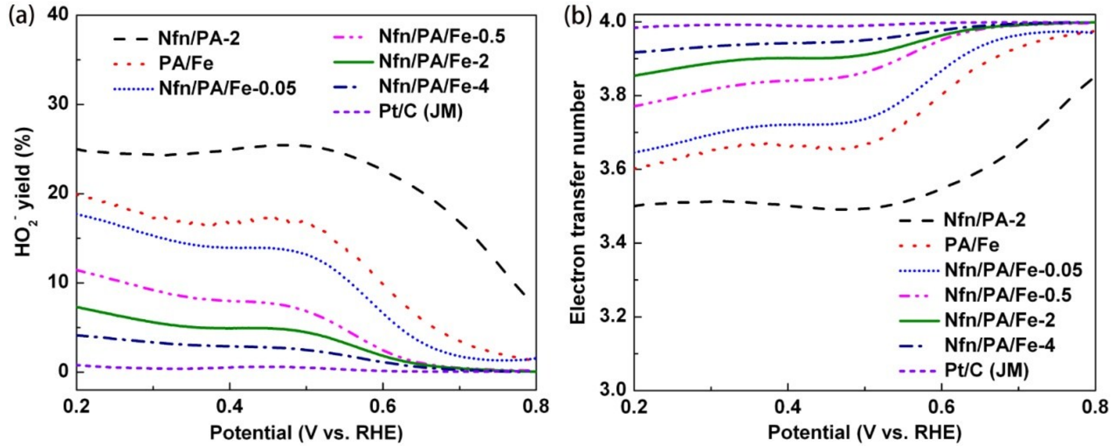

Fig. S7 (a) Yield of HO_2^- for Nfn/PA-2, PA/Fe, Nfn/PA/Fe-0.05, Nfn/PA/Fe-0.5, Nfn/PA/Fe-2, Nfn/PA/Fe-4 and Pt/C (JM); (b) Electron transfer number of Nfn/PA-2, PA/Fe, Nfn/PA/Fe-0.05, Nfn/PA/Fe-0.5, Nfn/PA/Fe-2, Nfn/PA/Fe-4 and Pt/C (JM).

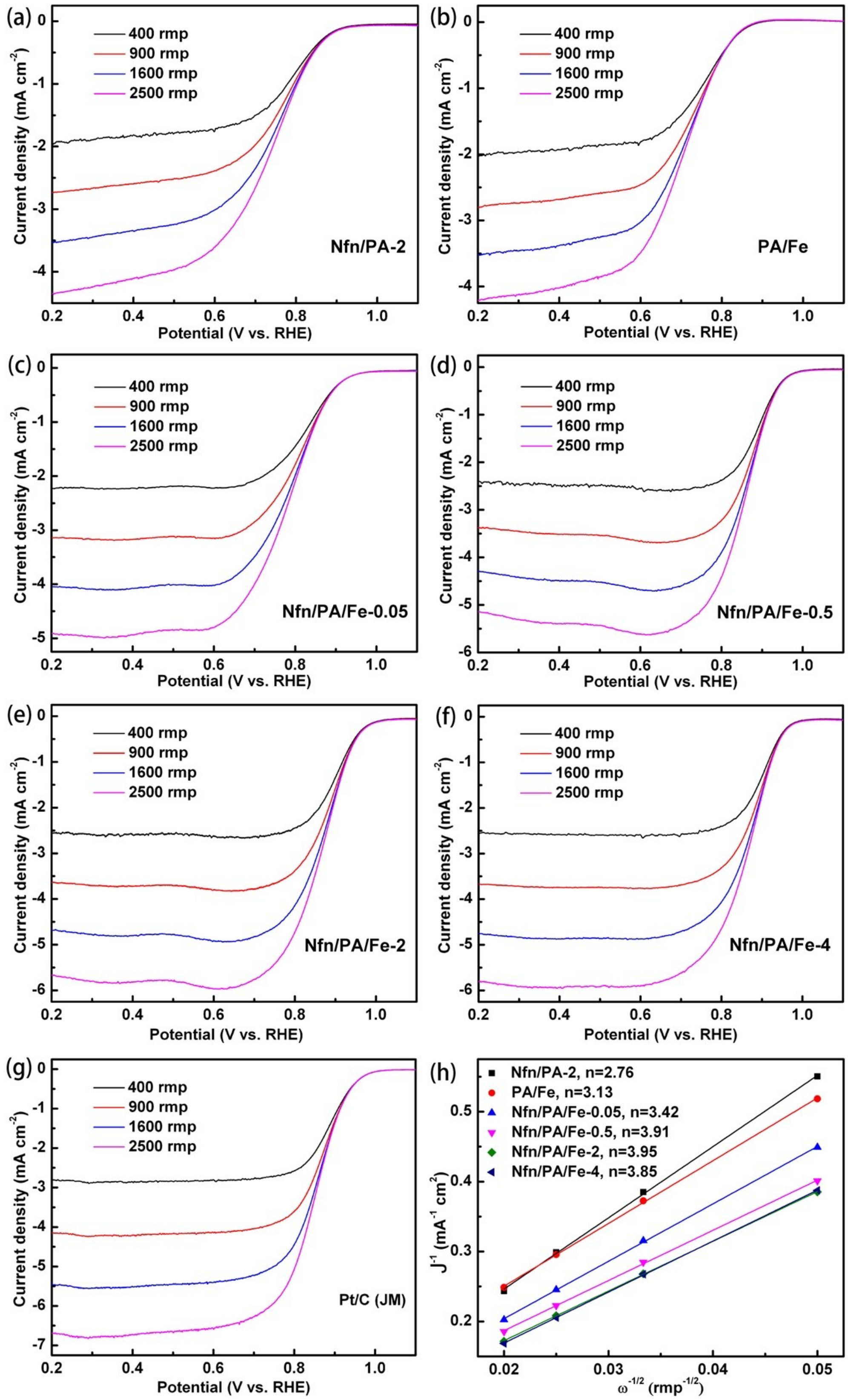

Fig. S8 ORR polarization curves of Nfn/PA-2 (a), PA/Fe (b), Nfn/PA/Fe-0.05 (c), Nfn/PA/Fe-0.5 (d), Nfn/PA/Fe-2 (e), Nfn/PA/Fe-4 (f), Pt/C (JM) (g) with various rotating rates in O_2-saturated 0.1M KOH electrolyte and the corresponding Koutechy-Levich plots at 0.4 V (h). Scan rate: 10 mV s^{-1}.

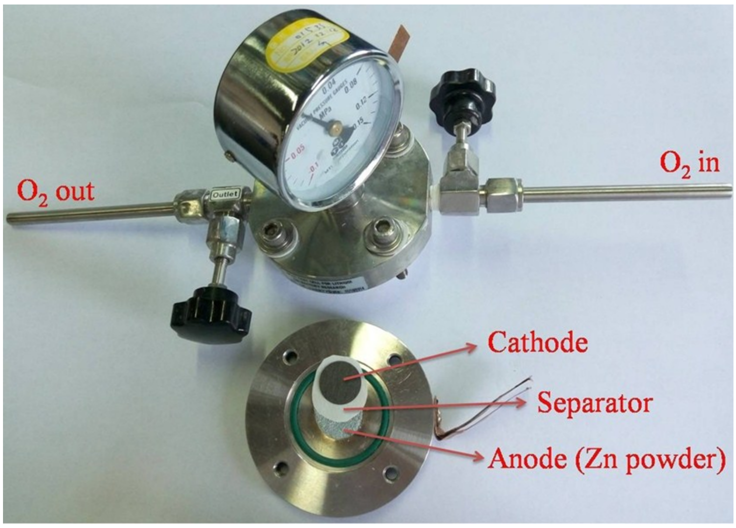

Fig. S9 A photo of the single cell to test Zn-air battery.

Table S1. RDE results for prepared catalysts and Pt/C, XPS and specific surface area data for prepared catalysts.

Sample	Onset potential (V vs. RHE)	Half wave potential(V vs. RHE)	Nitrogen content (at.%)					Weight loss (%)	BET (m^2 g^{-1})
			Total	$N_{pyridinic}$	$N_{graphitic}$	$N_{pyrrolic}$	$N_{oxidized}$		
Nfn/PA-2	0.931	0.757	5.88	1.17	3.31	0.597	0.805	85.7	1406
PA/Fe	0.906	0.720	3.43	0.709	2.07	0.236	0.414	81.1	545
Nfn/PA/Fe-0.05	0.961	0.798	4.38	0.842	2.52	0.422	0.601	79.1	740
Nfn/PA/Fe-0.5	0.988	0.869	5.77	1.66	2.68	0.387	1.05	79.4	1173
Nfn/PA/Fe-2	1.01	0.879	7.15	1.96	3.14	1.05	1.00	81.2	1325
Nfn/PA/Fe-4	0.991	0.876	5.34	0.954	2.52	0.502	1.36	85.8	1624
Pt/C (JM)	0.990	0.860							

Table S2. Summary of the oxygen reduction reaction activities, nitrogen contents and specific surface areas of our catalysts and other previously reported MNC catalysts.

Electrocatalysts	Catalyst Loading (mg cm^{-2})	Electrolyte	Half-wave Potential (V vs. RHE)	Nitrogen Content (at.%)	BET (m^2 g^{-1})	Pyrolysed Tempera-ture (°C)	Ref.
Meso/micro-PANI	0.1	0.1 M KOH	0.83	5.86	1190	900	S1
NPMC-900	0.15	0.1 M KOH	0.75	6.1	635.6	900	S2
NPMC-1000	0.15	0.1 M KOH	0.85	3.2	1548	1000	S2
Fe/N/G-0.3	0.6	0.1 M KOH	0.83	2.6	297	800	S3
CNT/(N–C)-800	0.1	0.1 M KOH	0.844	7.36	630	800	S4
CNT/(N–C)-900	0.1	0.1 M KOH	0.793	3.55	640	900	S4
N–S-GAs 900	0.425	0.1 M KOH	-0.24[a]	0.48	404.4	900	S5
CH-mel	0.487	0.1 M KOH	0.595	3.0	285.3	700	S6
FeN-HCS	0.5	0.1 M KOH	0.834	4.6[b]	103.7	900	S7
FeCoPc-C	0.4	0.1 M NaOH	0.85	2.62	361.3	900	S8
SN-OMC-900	0.1	0.1 M KOH	0.78	3.22	816.8	900	S9
Fe-N/G	0.05	0.1 M KOH	0.874[c]	5.21	393	900	S10
Nfn/PA/Fe-2	0.2	0.1 M KOH	0.879	7.15	1325	900	This
Nfn/PA/Fe-4	0.2	0.1 M KOH	0.876	5.34	1624	900	work

[a] vs. SCE

[b] wt.%

[c] onset potential

S1. H. W. Liang, X. Zhuang, S. Bruller, X. Feng and K. Mullen, *Nat. Commun.*, 2014, **5**, 4973.

S2. J. Zhang, Z. Zhao, Z. Xia and L. Dai, *Nat. Nano.*, 2015, **10**, 444-452.

S3. C. Dominguez, F. J. Perez-Alonso, M. A. Salam, S. A. Al-Thabaiti, M. A. Pena, L. Barrio and S. Rojas, *J. Mater. Chem. A*, 2015, **3**, 24487-24494.

S4. J.-C. Li, S.-Y. Zhao, P.-X. Hou, R.-P. Fang, C. Liu, J. Liang, J. Luan, X.-Y. Shan and H.-M. Cheng, *Nanoscale*, 2015, **7**, 19201-19206.

S5. M. Wu, Z. Dou, J. Chang and L. Cui, *RSC Adv.*, 2016, **6**, 22781-22790.

S6. M. K. Rybarczyk, M. Lieder and M. Jablonska, *RSC Adv.*, 2015, **5**, 44969-44977.

S7. Q. Gao, Q. Lai and Y. Liang, *RSC Adv.*, 2015, **5**, 103302-103307.

S8. S. Lee, D.-H. Kwak, S.-B. Han, E.-T. Hwang, M.-C. Kim, J.-Y. Lee, Y.-W. Lee and K.-W. Park, *Electrochim. Acta*, 2016, **191**, 805-812.

S9. X. Song, H. Ren, J. Ding, C. Wang, X. Yin and H. Wang, *Mater. Lett.*, 2015, **159**, 280-283.

S10. Q. Lai, Q. Su, Q. Gao, Y. Liang, Y. Wang, Z. Yang, X. Zhang, J. He and H. Tong, *ACS Appl. Mater. Interfaces*, 2015, **7**, 18170-18178.